Science of the Total Environment 653 (2019) 1522–1531

Contents lists available at ScienceDirect

Science of the Total Environment

journal homepage: www.elsevier.com/locate/scitotenv

Wave farm impacts on coastal flooding under sea-level rise: A case study in southern Spain

Rafael J. Bergillos[a,b,*], Cristobal Rodriguez-Delgado[c], Gregorio Iglesias[c,d]

[a] Andalusian Institute for Earth System Research, University of Granada, Avda. del Mediterráneo, s/n, Granada 18006, Spain
[b] Hydraulic Engineering Area, Department of Agronomy, University of Córdoba, Rabanales Campus, Leonardo Da Vinci Building, Córdoba 14071, Spain
[c] School of Engineering, University of Plymouth, Plymouth PL4 8AA, UK
[d] MaREI, Environmental Research Institute & School of Engineering, University College Cork, College Road, Cork, Ireland

HIGHLIGHTS

- Assessment of the wave farm impacts on coastal flooding on a gravel-dominated beach.
- Three sea-level rise scenarios are modelled and analysed with and without wave farm.
- Reductions in breaking wave height, total run-up and flooded area induced by the farm.
- Wave farms contribute to reduce carbon emissions, beach erosion and coastal flooding.

GRAPHICAL ABSTRACT

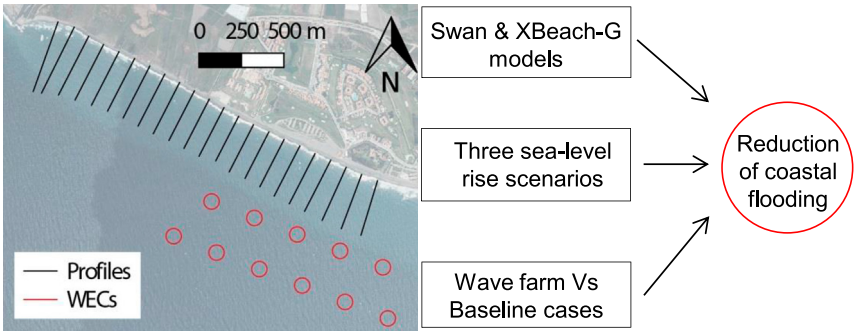

ARTICLE INFO

Article history:
Received 15 September 2018
Received in revised form 15 October 2018
Accepted 30 October 2018
Available online 3 November 2018

Editor: José Virgílio Cruz

Keywords:
Coastal flooding
Global warming
Sea-level rise
Renewable energy
Wave farm
Coastal defence

ABSTRACT

Coastal flooding, already an acute problem in many parts of the world, will be exacerbated in the near future by the sea level rise induced by climate change. The influence of wave farms, i.e., arrays of wave energy converters, on coastal processes, in particular sediment transport patterns, has been analysed in recent works; however, their influence on coastal flooding has not been addressed so far. The objective of this work is to investigate whether a wave farm can provide some protection from flooding on the coast in its lee through a case study: a gravel-dominated beach in southern Spain (Playa Granada). We consider three sea-level rise (SLR) scenarios: the present situation (SLR0), an optimistic projection (SLR1) and a pessimistic projection (SLR2). Two state-of-the-art numerical models, SWAN and XBeach-G, are applied to determine the wave propagation patterns, total run-up and flooded dry beach area. The results indicate that the absorption of wave power by the wave farm affects wave propagation in its lee and, in particular, wave heights, with alongshore-averaged reductions in breaking wave heights about 10% (25%) under westerly (easterly) storms. These lower significant wave heights, in turn, result in alongshore-averaged run-up reductions for the three scenarios, which decreases with increasing SLR values from 5.9% (6.8%) to 1.5% (5.1%) for western (eastern) storms. Importantly, the dry beach area flooded under westerly (easterly) storms is also reduced by 5.7% (3.2%), 3.3% (4.9%) and 1.99% (4.5%) in scenarios SLR0, SLR1 and SLR2, respectively. These findings prove that a wave farm can actually reduce coastal flooding on its leeward coast.

1. Introduction

Over the past few decades, the demand for energy worldwide has grown massively and has been mainly met by fossil fuels

* Corresponding author.
E-mail addresses: rbergillos@ugr.es, rafael.bergillos@uco.es (R.J. Bergillos).

https://doi.org/10.1016/j.scitotenv.2018.10.422
0048-9697/

(Asif and Muneer, 2007; Shafiee and Topal, 2009; Gaete-Morales et al., 2018). However, these fossil fuels induce acute damage to the environment and contribute to aggravate the negative consequences of climate change (Atilgan and Azapagic, 2015; Feng et al., 2018). Thus, the development and usage of carbon-free energy sources are increasingly necessary (European Commission, 2007). Wave energy is, among the renewable sources of energy, one of the most advisable due to its huge availability and potential (Cornett, 2008; Cruz, 2008), and its relatively low impacts on the environment with respect to other carbon-free energy sources (Clément et al., 2002; Palha et al., 2010).

Notable progress on wave energy has been achieved recently along the following research lines: (i) the characterisation of the wave energy resource (Iglesias and Carballo, 2011; Carballo et al., 2015; López et al., 2015c; Silva et al., 2015; Viviano et al., 2016; Medina-López et al., 2017; López-Ruiz et al., 2018a,b), (ii) the development and improvement of different types of wave energy technologies (de O. Falcão, 2007; Margheritini et al., 2009; Fernandez et al., 2012; López and Iglesias, 2014; López et al., 2015a,b, 2014; Contestabile et al., 2017b), (iii) the analysis of potentially viable locations (Carballo et al., 2014; Iuppa et al., 2015; López-Ruiz et al., 2016), (iv) the joint assessment of wave and other renewable energy sources (Astariz et al., 2015a; Astariz and Iglesias, 2015b, 2016a; Pérez-Collazo et al., 2015) and (v) the study of economic indicators (Astariz et al., 2015b; Astariz and Iglesias, 2015a, 2016b; Contestabile et al., 2017a).

Wave farms, composed by arrays of wave energy converters (WECs), have been proven to be capable of performing the dual function of generating carbon-free energy and protecting sandy coastlines against erosion (Millar et al., 2007; Mendoza et al., 2014; Abanades et al., 2018, 2014a,b, 2015). Recent works have also demonstrated that wave farms mitigate erosion issues on mixed and gravel-dominated coasts (Bergillos et al., 2018a; Rodriguez-Delgado et al., 2019, 2018a,b). The dual function of wave farms is key for the development of this energy source, as many coasts across the world are experiencing erosion issues mainly due to human intervention (Aragonés et al., 2016; Pagán et al., 2017) and climate change (Sánchez-Arcilla et al., 2016). However, the impacts of wave farms on coastal flooding considering the effects of sea-level rise (SLR) have not been fully addressed so far.

The overall goal of this paper is to investigate the influence of a wave farm on wave patterns at the nearshore region, total run-up (including water level) and flooded area under three SLR scenarios: the present situation (SLR0), and optimistic (SLR1) and pessimistic (SLR2) projections proposed by Intergovernmental Panel on Climate Change (2014). For this purpose, a wave model (SWAN) and a storm response model (XBeach-G) were jointly applied to two case studies (with and without wave farm) under storm conditions. The following sections detail the study area, the wave farm location and geometry, the analysed sea states and sea-level rise scenarios, the implementation of SWAN and XBeach-G, the results obtained and the conclusions drawn.

2. Study area

Playa Granada is a 3-km-long gravel-dominated beach located on the southern coast of Spain that faces the Mediterranean Sea (Fig. 1a). Limited to the west by the Guadalfeo River mouth and to the east by Punta del Santo (a shoreline horn located at the former location of the river mouth), this beach belongs to the Guadalfeo deltaic coast, extending between Salobreña Rock and the Port of Motril (Fig. 1b).

The Guadalfeo River contributes most of the sediment to the beach (Bergillos et al., 2016d, 2015b). Its basin covers an area of 1252 km^2, including the highest peaks in the Iberian Peninsula (~3400 m.a.s.l.), and the river is associated with one of the most high-energy drainage systems along the Spanish Mediterranean coast (Millares et al., 2014). The river was dammed 19 km upstream from its mouth in 2004, regulating 85% of the basin run-off (Losada et al., 2011).

As a consequence of river damming, the delta currently experiences severe erosion problems and frequent coastal flooding events (Fig. 2). The stretch of Playa Granada has been particularly affected, with more severe coastline retreat in recent years than both the western (between Salobreña Rock and Guadalfeo River Mouth)

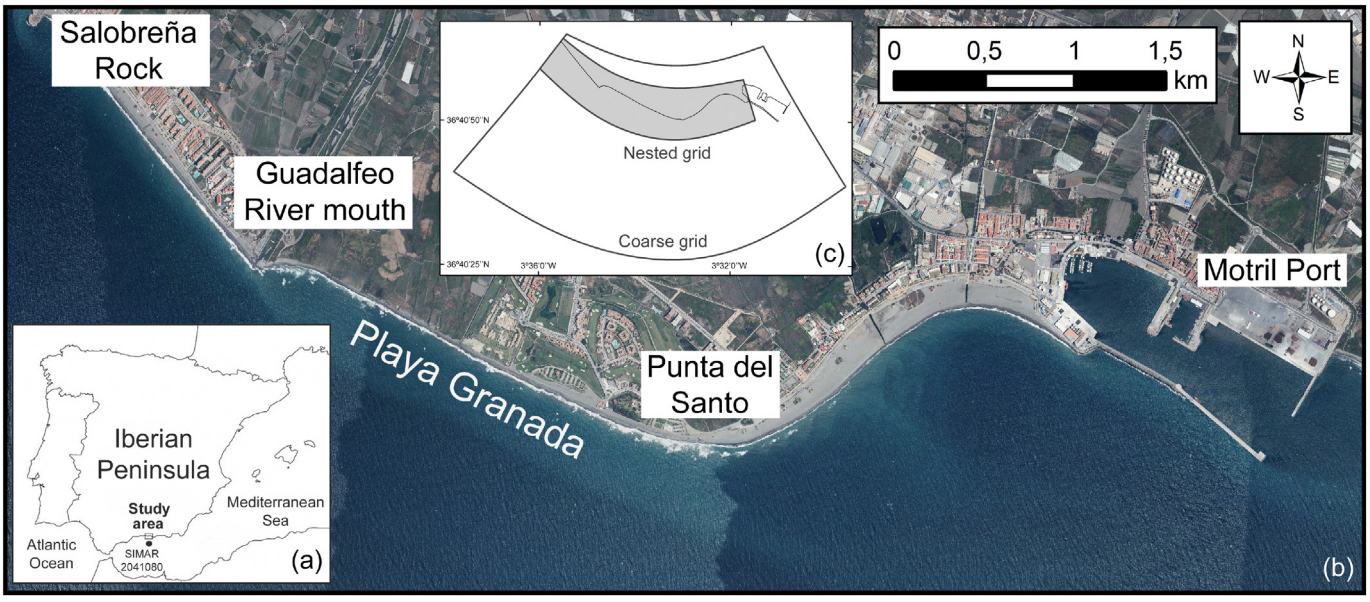

Fig. 1. (a) Location of the study area in southern Spain, (b) plan view of the deltaic coast, indicating the studied stretch of beach (Playa Granada), (c) contours of the numerical grids used in the SWAN model.

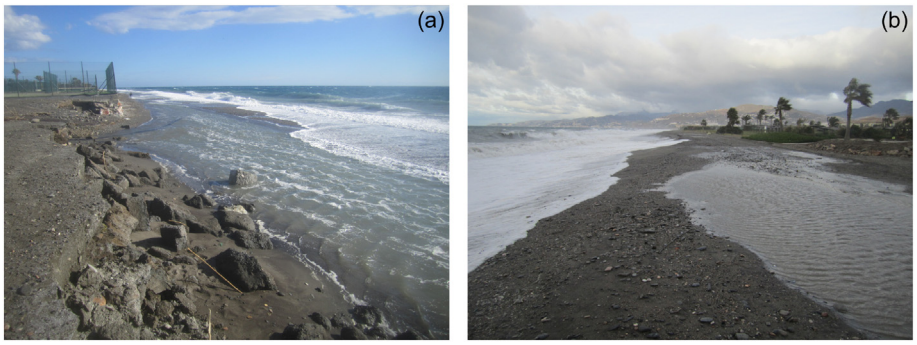

Fig. 2. Examples of coastal flooding events in Playa Granada.
(Sources: Rodriguez-Delgado et al. (2019) and Bergillos et al. (2017a). Reproduced with permission of Elsevier).

and eastern (between Punta del Santo and Motril Port) stretches (Bergillos et al., 2016a, 2015a).

Playa Granada comprises a wide range of activities and land uses, such as farming settlements, an exclusive hotel complex, residential properties that are primarily summer homes, golf fields and restaurants. Hence, this stretch of beach has high environmental and tourism value, and its exploitation requires a large area of dry beach (Félix et al., 2012). For this reason, artificial nourishment projects have been frequent since the river damming (Bergillos et al., 2015b). However, the success of these interventions has been very limited (Bergillos et al., 2018b, 2017b).

This micro-tidal coast is subjected to extra-tropical Atlantic cyclones and Mediterranean storms (Ortega-Sánchez et al., 2017). Thus, the wave climate is bidirectional, with waves coming from the west-southwest (extra-tropical cyclones), and east-southeast (Mediterranean storms). The deep-water significant wave height with non-exceedance probabilities of 50%, 90% and 99.9% are 0.5 m, 1.2 m and 3.1 m, respectively (Bergillos et al., 2016c). The astronomical tidal range is 0.6 m and storm surges can exceed 0.5 m (Bergillos et al., 2017a).

3. Methods

3.1. Wave farm location and geometry

In order to analyse the effects of a wave farm on wave propagation and coastal flooding, we selected the wave farm location indicated in Fig. 3, with the geometrical centre situated at 30 m water depth. This position was found to be optimum in terms of both wave energy availability (López-Ruiz et al., 2016) and coastline protection (Rodriguez-Delgado et al., 2018b).

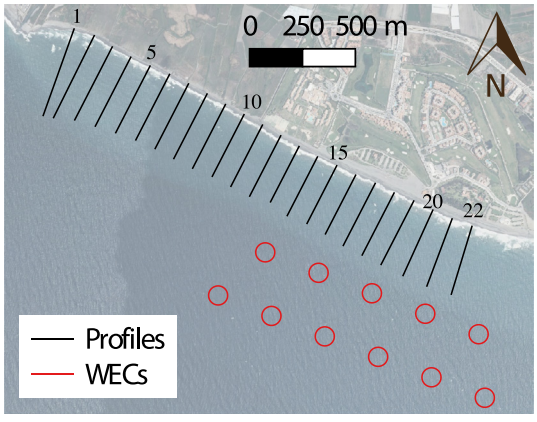

Fig. 3. Location of the studied beach profiles (1–22, in black) and wave energy converter farm (in red).

The wave farm layout consisted of eleven WaveCat devices, distributed in two rows and with an inter-device spacing equal to 180 m (Fig. 3). WaveCat is a type of overtopping WEC composed by two hulls connected by the stern, with a distance between them commonly equal to 90 m (Carballo and Iglesias, 2013). The efficiency of WaveCat and the wave farm layout selected for coastal defence purposes has been widely demonstrated in previous works (e.g. Rodriguez-Delgado et al., 2019; Rodriguez-Delgado et al., 2018a).

3.2. Sea states and sea-level rise scenarios

The effects of western and eastern storms (prevailing wave directions at the study site) were simulated by means of the SWAN and XBeach-G models. The input wave conditions for SWAN were deep-water significant wave height equal to 3.1 m, spectral peak period equal to 8.4 s (the most common value at the study area for storm conditions) and deep-water wave directions equal to 238° (107°) for the westerly (easterly) storm. These are the most frequent wave directions at the study site under western and eastern storm conditions, respectively. These sea states were modelled under high tide conditions and for a storm surge of 0.5 m (typical value in the study area under storm conditions).

These storms were modelled for two case studies and three SLR scenarios. The two study cases correspond to the natural, no-farm situation (i.e., baseline case study) and the situation including the wave farm described in Section 3.1 (i.e., wave farm case study). On the other hand, the three tested SLR scenarios were: present situation (SLR0) and SLR associated to the representative concentration pathways 4.5 and 8.5 at the study area according to Intergovernmental Panel on Climate Change (2014), which represent optimistic (SLR1 = 0.45 m) and pessimistic (SLR2 = 0.65 m) projections by 2100, respectively.

3.3. SWAN model

The spectral wave model SWAN (Holthuijsen et al., 1993) was used to propagate the two storm sea states from deep water to the nearshore region under the three SLR scenarios described in the previous section. The SWAN model was validated for the study area by means of comparison with hydrodynamic measurements collected by two ADCPs during a continuous 41-day field survey (Bergillos et al., 2017b). In this work, we used the computational grids shown in Fig. 1c, which were also employed for the calibration of the model.

The WaveCat devices were modelled in SWAN as artificial obstacles. The adopted values of the reflection and transmission coefficients were 0.43 and 0.76, respectively, according to those measured for this type of WEC during laboratory experiments by Fernandez et al. (2012). The results of the SWAN model were used to quantify the

variations in wave propagation patterns and breaking wave height values induced by the presence of the wave farm. They were also employed to provide the input conditions for the XBeach-G model, as detailed in the following section.

3.4. XBeach-G model

The storm impact model XBeach-G, which was specifically developed for reproducing the storm hydrodynamics, hydrology and morphodynamics of gravel-dominated beaches (McCall et al., 2015, 2014), was applied to quantify the values of the total run-up (including water level) under the storm conditions and sea-level rise scenarios detailed in Section 3.2. The XBeach-G model was validated for the study area by means of comparison with morphological data measured before and after storm events (Bergillos et al., 2016b, 2017a).

The XBeach-G model was applied to 22 equally-spaced beach profiles (one per 100 m) along the studied stretch of beach (Fig. 3). The offshore boundary conditions for XBeach-G were computed through the results of SWAN at a water depth equal to 10 m for all the beach profiles. This value of the offshore depth is in agreement with all the model requirements (Deltares, 2014). On the other hand, the landside boundaries were variables alongshore depending on the type of land use located landward of the beach profiles (farming settlements, hotel complex, golf field or residential properties, see Fig. 3).

The results of the XBeach-G model were employed to compute the maximum values of total run-up and flooded cross-shore distance in every beach profile. The values of total flooded area along the section of Playa Granada for the analysed study cases and SLR scenarios were also obtained.

4. Results and discussion

4.1. Wave propagation: breaking wave height

The absorption and dissipation of energy due to the presence of a wave farm induce modifications in wave propagation patterns in the lee of the farm. Fig. 4 depicts the variations in significant wave height induced by the farm with respect to the baseline case study for the three SLR scenarios. Under westerly storm conditions, it is observed that the wave height is significantly reduced behind the devices; this reduction is focused on the eastern part of Playa Granada (Fig. 4 a1–c1). The reduction in wave height is even greater under eastern storms and is extended along most of the studied coastline section

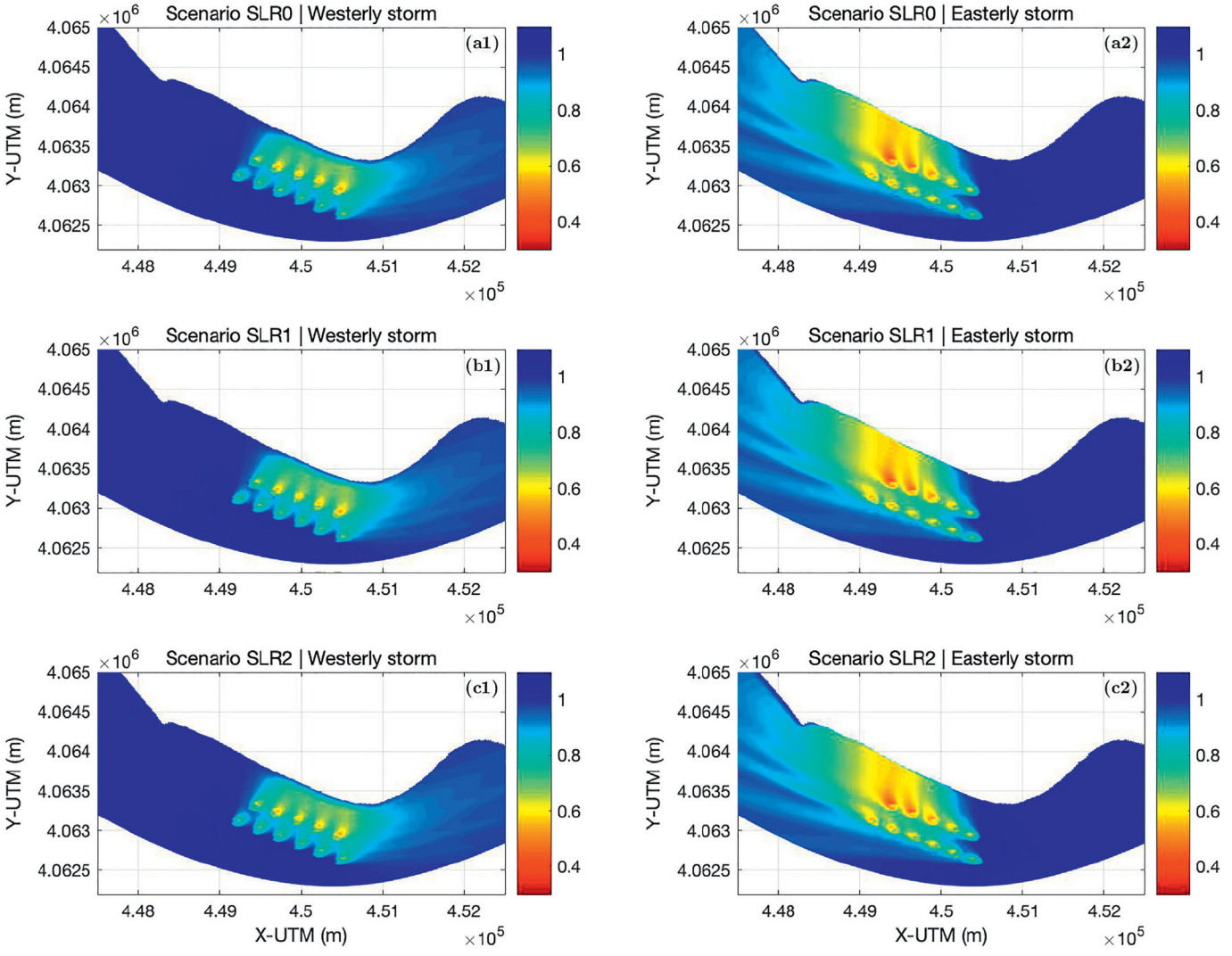

Fig. 4. Ratio of significant wave height for the wave farm case study with respect to the baseline for scenarios SLR0 (a), SLR1 (b) and SLR2 (c) under westerly (1) and easterly (2) storms.

(Fig. 4 a2–c2). For both incoming directions, the reduction values are slightly higher in scenario SLR0 than in scenarios SLR1 and SLR2.

These reductions generate changes in the significant wave height at breaking, as it is depicted in Fig. 5. Under westerly storms, the presence of the wave farm leads to a reduction in the breaking wave height in the eastern part of Playa Granada, which is in agreement with the plan view distributions of wave height variations shown in Fig. 4. The reduction peak values are equal to 24.1% (SLR0), 26.4% (SLR1) and 25.8% (SLR2), whereas the alongshore-averaged reductions in Playa Granada are 9.3%, 9.8% and 9.9%, respectively. Conversely, in the west side of the farm, the significant wave height at breaking of the wave farm case study is slightly increased with respect to the baseline (Fig. 5 a1–b1). This is influenced by the reflection and diffraction processes induced by the devices.

Under eastern storm conditions, the reductions in significant wave height are concentrated in the western part of Playa Granada and extended along a larger distance than under westerly storms, with maximum reductions up to 42%, 40.3% and 41.9% for scenarios SLR0, SLR1 and SLR2, respectively. In this case, increases in wave height values are observed to the east of the wave farm location, also influenced by the WEC-induced diffraction and reflection processes (Fig. 5 a2–b2). Under these wave conditions, the alongshore-averaged reductions induced by the farm in scenarios SLR0, SLR1 and SLR2 are equal to 24.8%, 25.7% and 26.3%, respectively.

In both case studies and for both wave directions, it is observed that, in general, the greater the SLR, the greater the breaking significant wave heights. Thus, global warming will not only induce SLR, but these variations in sea level will also lead to greater wave height and power in the breaking zone. Both the SLR and the increase in breaking wave height will contribute to coastal flooding, as explained below.

4.2. Total run-up

As indicated in Section 3.4, the total run-up (including water level) was computed with the XBeach-G model in the 22 beach profiles shown in Fig. 3. The results for the wave directions, case studies and SLR scenarios modelled are shown in Figs. 6 and 7.

Under western storms, the presence of the wave farm reduces the total run-up, from profile 12 to profile 22, up to 14.1%, 8.7% and 8.3% in scenarios SLR0, SLR1 and SLR2, respectively. The alongshore-averaged reductions in total run-up along the studied stretch of beach for scenarios SLR0, SLR1 and SLR2 are equal to 5.9%, 2.6% and 1.5%, respectively. Thus, the reductions are more significant in scenario SLR0 than those in the two scenarios of representative concentration pathways (Fig. 7). The total run-up in the wave farm case study is slightly increased with respect to the baseline in the western part of Playa Granada (Figs. 6 and 7); this is influenced by the greater breaking significant wave heights at this location for the wave farm case (Fig. 5).

On the other hand, under eastern storm conditions, the total run-up is reduced due to the presence of the wave farm along most of the studied stretch of beach, with only some minor increases in its eastern boundary (Figs. 6 and 7). The farm leads to maximum (alongshore-averaged) reductions in total run-up of 13.6% (6.8%), 12% (6.1%) and 10.1% (5.1%) for scenarios SLR0, SLR1 and SLR2, respectively. Under these wave conditions, the total run-up values are generally lower than those under western storms. This is due to the orientation of the coastline in Playa Granada, which is almost normal to the prevailing western direction under high energy conditions.

The results for all the wave conditions, study cases and SLR scenarios detailed in this section highlight the efficiency of wave farms composed by WaveCat devices for the reduction of total run-up values. This has important implications for the mitigation of coastal flooding events, as it is indicated in Sections 4.3 and 4.4.

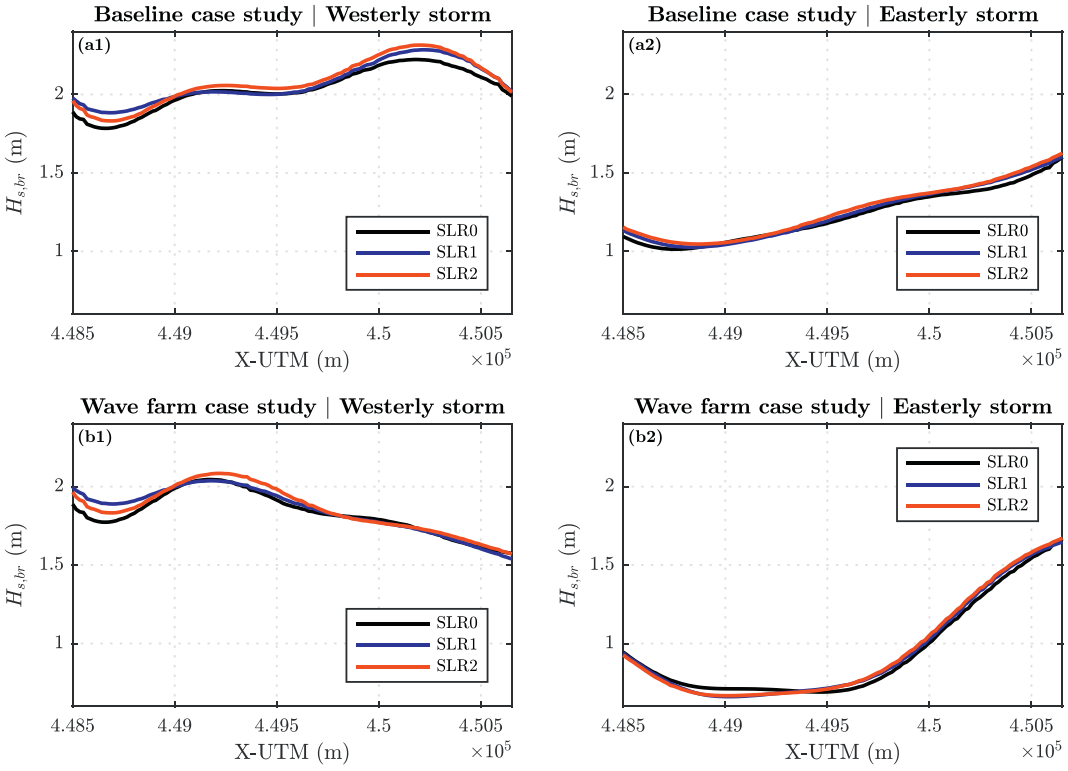

Fig. 5. Significant wave height at breaking along the studied stretch of beach for the baseline (a) and wave farm (b) case studies under westerly (1) and easterly (2) storms. Scenarios SLR0, SLR1 and SLR2.

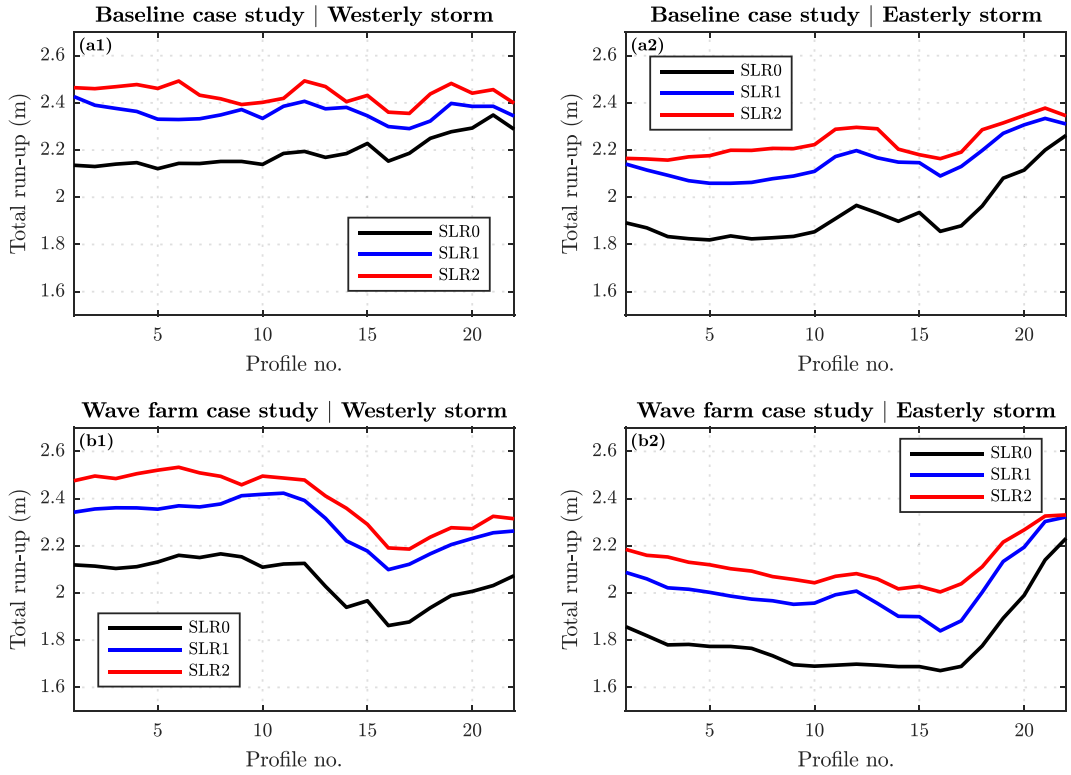

Fig. 6. Total run-up values in the studied beach profiles for the baseline (a) and wave farm (b) case studies under westerly (1) and easterly (2) storms. Scenarios SLR0, SLR1 and SLR2.

4.3. Flooded cross-shore distances

This section reports the flooded cross-shore distances for the wave conditions, study cases and SLR scenarios analysed. These flooded distances, which are influenced by both the total run-up values depicted in Fig. 6 and the morphologies of the emerged beach profiles, are shown in Fig. 8. For westerly storms, reductions in flooded distances occur between profiles 11 and 22 in scenario SLR0, and between profiles 17 and 22 in scenarios SLR1 and SLR2 (Fig. 9). This is influenced by the SLR values in scenarios SLR1 and SLR2, which lead to an overwash of the whole beach for the case studies with and without wave farm in profiles 1–16. The maximum (alongshore-averaged) reductions in flooded cross-shore distances induced by the wave farm under western storm conditions for scenarios SLR0, SLR1 and SLR2 are equal to 16.2% (4.8%), 15.7% (2.5%) and 10.1% (1.5%), respectively.

Under easterly storms, the flooded distance diminishes due to the wave farm in profiles 11 to 21 for the three SLR scenarios (Figs. 7 and 8). In profiles 1 to 10, the beach is overwashed in each scenario in the same way as for westerly storms. This is due to the lower dry beach area in this stretch, which is closer to the river mouth and has experienced greater values of shoreline retreat in recent years due to river regulation (Bergillos et al., 2016d). For eastern storm conditions, the maximum (alongshore-averaged) farm-induced reductions in flooded cross-shore distances in scenarios SLR0, SLR1 and SLR2 are equal to 11.8% (3.1%), 12.5% (4.4%) and 12.2% (3.8%), respectively. The

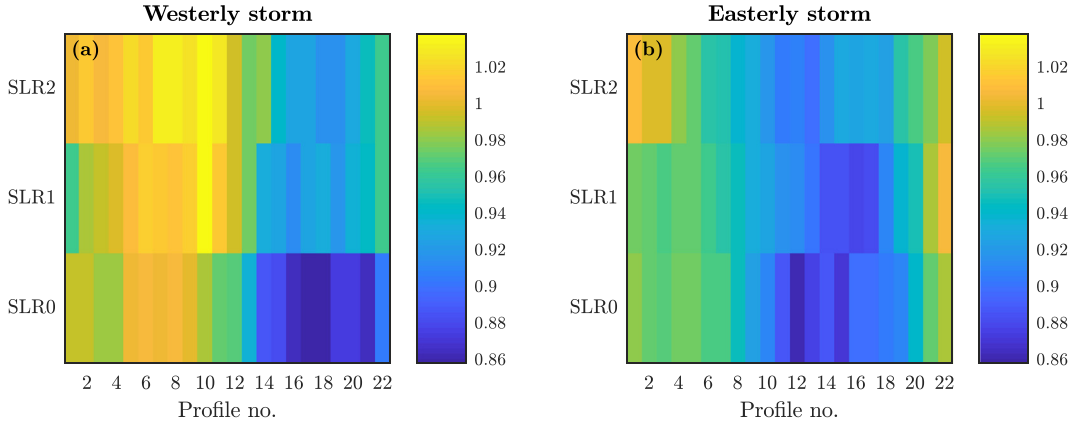

Fig. 7. Ratio of total run-up for the wave farm case study with respect to the baseline under westerly (a) and easterly (b) storms. Scenarios SLR0, SLR1 and SLR2.

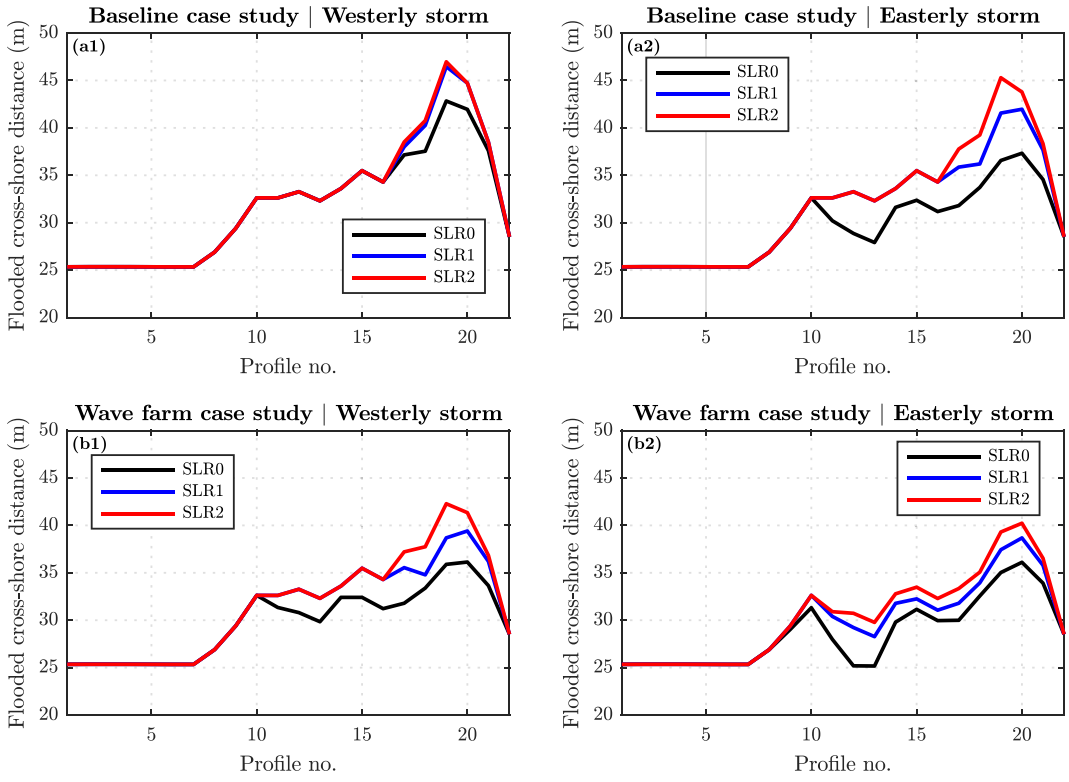

Fig. 8. Flooded cross-shore distances in the studied beach profiles for the baseline (a) and wave farm (b) case studies under westerly (1) and easterly (2) storms. Scenarios SLR0, SLR1 and SLR2.

reductions for these wave conditions are extended along the whole urbanized stretch of beach, with maximum values of 6 m; whereas under westerly storms the reductions are concentrated in the eastern part of Playa Granada, reaching values up to 7.8 m (Figs. 9 and 10).

4.4. Flooded area

Fig. 11 represents the total flooded dry beach areas in the baseline and wave farm study cases for the three SLR scenarios under both western and eastern storm conditions. Under westerly storms, the reductions in coastal flooding induced by the wave farm are equal to 3976.4 m^2 (5.7%), 2331.5 m^2 (3.3%) and 1404.1 m^2 (1.99%) for scenarios SLR0, SLR1 and SLR2, respectively. Thus, the reduction in flooded area decreases with increasing SLR values. This trend is influenced by the SLR-induced overwash of the whole dry beach in both study cases for scenarios SLR1 and SLR2 at some locations that are not overwashed for scenario SLR0 (profiles 11–16, see Figs. 8 and 9). In any case, the wave farm provides protection against coastal flooding events in all the SLR scenarios.

For eastern storm conditions, the differences in flooded dry beach area between the baseline and wave farm case studies in scenarios SLR0, SLR1 and SLR2 are equal to 2095.3 m^2 (3.2%), 3419.4 m^2 (4.9%) and 3155.5 m^2 (4.5%), respectively. In this case, the maximum reduction takes place in scenario SLR1 since some parts of the beach are only fully overwashed in both study cases for scenario SLR2, reducing the farm-induced differences in flooded dry beach area for this latter scenario. In scenarios SLR1 and SLR2, the reductions are significantly greater under easterly storms, so that a wave farm would

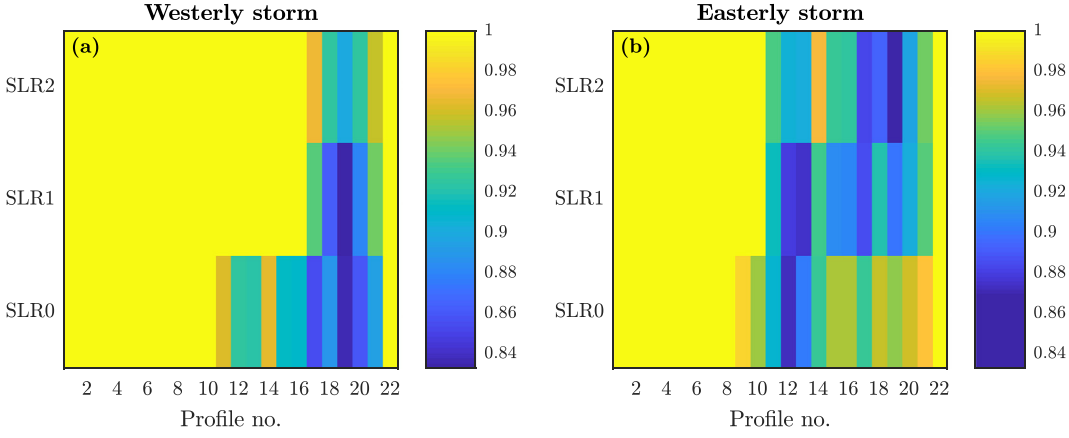

Fig. 9. Ratio of flooded cross-shore distance for the wave farm case study with respect to the baseline under westerly (a) and easterly (b) storms. Scenarios SLR0, SLR1 and SLR2.

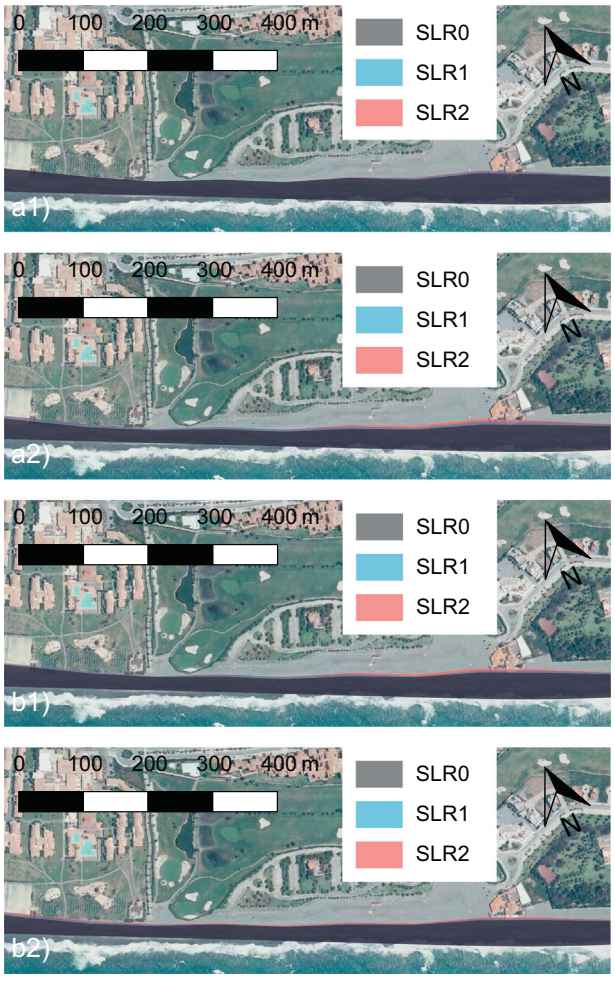

Fig. 10. Flooded area along the urbanized stretch of beach for the baseline (a) and wave farm (b) case studies under westerly (1) and easterly (2) storms. Scenarios SLR0, SLR1 and SLR2.

be particularly helpful to reduce the flooded areas associated to the IPCC projections for these wave conditions.

Under both wave directions, the coastal flooding increases with increasing values of SLR for both study cases, being the flooded area in the wave farm case study lower than in the baseline for all the SLR scenarios. Thus, these results indicate that a wave farm would contribute to mitigate coastal flooding issues in Playa Granada, which will be more severe in the coming years due to the expected SLR induced by global warming.

5. Conclusions

The study of wave energy has received increasing research attention in the past few years and recent works have highlighted the dual function of wave farms as carbon-free energy generators and coastal protection elements against erosion. However, the effects of wave farms on coastal flooding had not been analysed so far. This paper investigates the efficiency of a wave farm in reducing storm-induced coastal flooding on a gravel-dominated beach under three sea-level rise scenarios: present situation (SLR0), optimistic projection (SLR1) and pessimistic projection (SLR2).

With this purpose, the SWAN and XBeach-G models, previously validated for the study site, were coupled and applied to 22 beach profiles in order to assess wave propagation patterns, total run-up values (including water level), flooded cross-shore distances and total flooded area for the prevailing storm directions (SW and SE) and the three aforementioned SLR scenarios. The results were compared to the baseline (no farm) case study.

In terms of wave propagation patterns, under westerly storms, the WEC farm modifies significantly the wave height leeward of the devices and leads to a reduction in significant wave height at breaking in the eastern part of the study area. Conversely, the reductions in breaking wave height under easterly storms extend along most of the study area, reaching the maximum reduction values in the western part. The breaking significant wave heights are slightly increased with respect to the baseline to the west (east) of the wave farm under westerly (easterly) storms; this is influenced by the diffraction and reflection processes induced by the WECs.

The total run-up is reduced in the central and eastern parts of the beach under western storms; whereas under eastern storm conditions the total run-up decreases along most of the study area, with total run-up values generally lower than those under western storms. This is explained by the shoreline orientation in Playa Granada, which is almost normal to the incoming westerly waves. The total run-up is also slightly increased with respect to the baseline under westerly (easterly) storm waves in the western (eastern) part of the beach, induced by the greater breaking significant wave heights at these locations for the wave farm case.

Finally, flooded cross-shore distances are also reduced by the farm along the studied coastline section for both wave directions.

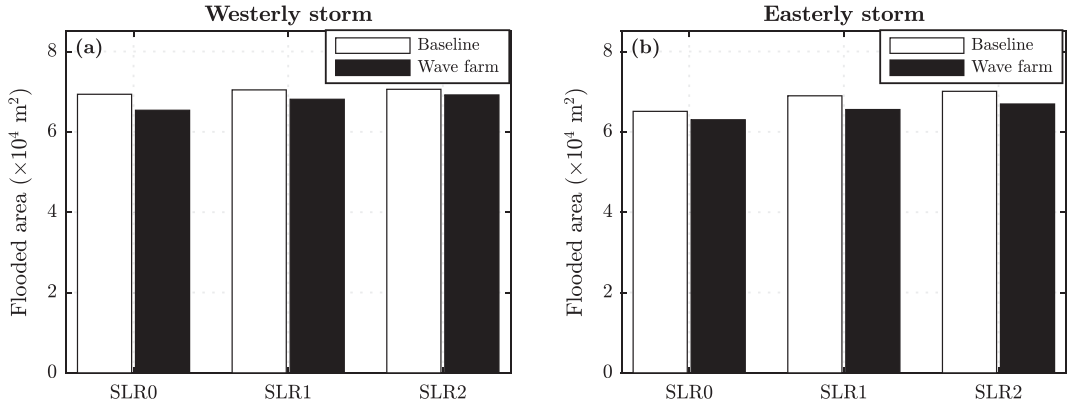

Fig. 11. Total flooded area in the baseline and wave farm case studies for scenarios SLR0, SLR1 and SLR2 under westerly (a) and easterly (b) storms.

The farm-induced decreases in flooded dry beach area under westerly (easterly) storms are equal to 5.7% (3.2%), 3.3% (4.9%) and 1.99% (4.5%) in scenarios SLR0, SLR1 and SLR2, respectively.

The results of the present paper highlight that a wave farm can be used not only for purposes of renewable energy generation and protection against erosion, but also to mitigate coastal flooding. These findings are especially relevant due to the sea-level rise expected in the coming decades associated to climate change. Future research efforts are required to assess the wave farm impacts on coastal flooding taking into account, apart from sea-level rise, other consequences of global warming, such as the variations in wave climate (Hemer et al., 2013; Vousdoukas et al., 2016).

Acknowledgments

This paper was carried out in the framework of the Coastal, Ocean and Sediment Transport (COaST) Engineering Research Group (University of Plymouth, UK) and the research grants WAVEIMPACT (PCIG-13-GA-2013-618556, European Commission, Marie Curie fellowship, fellow GI) and ICE (Intelligent Community Energy, European Commission, Contract no. 5025). RB was partly funded by the University of Granada through *Programa Contratos Puente 2017* and the *Ministerio de Ciencia, Innovación y Universidades* through *Programa Juan de la Cierva 2017* (Research contract FJCI-2017-31781). Wave, sea-level rise, bathymetric and DEM data were provided by *Puertos del Estado* (Spain), *Universität Hamburg* (Germany), *Ministerio de Agricultura, Pesca y Alimentación* (Spain) and *Instituto Geográfico Nacional* (Spain), respectively. The helpful suggestions of three anonymous reviewers are acknowledged.

References

Abanades, J., Flor-Blanco, G., Flor, G., Iglesias, G., 2018. Dual wave farms for energy production and coastal protection. Ocean Coast. Manag. 160, 18–29.
Abanades, J., Greaves, D., Iglesias, G., 2014a. Coastal defence through wave farms. Coast. Eng. 91, 299–307.
Abanades, J., Greaves, D., Iglesias, G., 2014b. Wave farm impact on the beach profile: a case study. Coast. Eng. 86, 36–44.
Abanades, J., Greaves, D., Iglesias, G., 2015. Coastal defence using wave farms: the role of farm-to-coast distance. Renew. Energy 75, 572–582.
Aragonés, L., Pagán, J., López, M., García-Barba, J., 2016. The impacts of Segura River (Spain) channelization on the coastal seabed. Sci. Total Environ. 543, 493–504.
Asif, M., Muneer, T., 2007. Energy supply, its demand and security issues for developed and emerging economies. Renew. Sust. Energ. Rev. 11, 1388–1413.
Astariz, S., Abanades, J., Perez-Collazo, C., Iglesias, G., 2015a. Improving wind farm accessibility for operation and maintenance through a co-located wave farm: influence of layout and wave climate. Energy Convers. Manag. 95, 229–241.
Astariz, S., Vazquez, A., Iglesias, G., 2015b. Evaluation and comparison of the levelized cost of tidal, wave, and offshore wind energy. J. Renew. Sust. Energy 7, 053112.
Astariz, S., Iglesias, G., 2015a. The economics of wave energy: a review. Renew. Sust. Energ. Rev. 45, 397–408.
Astariz, S., Iglesias, G., 2015b. Enhancing wave energy competitiveness through co-located wind and wave energy farms. A review on the shadow effect. Energies 8, 7344–7366.
Astariz, S., Iglesias, G., 2016a. Output power smoothing and reduced downtime period by combined wind and wave energy farms. Energy 97, 69–81.
Astariz, S., Iglesias, G., 2016b. Wave energy vs. other energy sources: a reassessment of the economics. Int. J. Green Energy 13, 747–755.
Atilgan, B., Azapagic, A., 2015. Life cycle environmental impacts of electricity from fossil fuels in Turkey. J. Clean. Prod. 106, 555–564.
Bergillos, R.J., López-Ruiz, A., Medina-López, E., Moñino, A., Ortega-Sánchez, M., 2018a. The role of wave energy converter farms on coastal protection in eroding deltas, Guadalfeo, southern Spain. J. Clean. Prod. 171, 356–367.
Bergillos, R.J., López-Ruiz, A., Principal-Gómez, D., Ortega-Sánchez, M., 2018b. An integrated methodology to forecast the efficiency of nourishment strategies in eroding deltas. Sci. Total Environ. 613-614, 1175–1184.
Bergillos, R.J., López-Ruiz, A., Ortega-Sánchez, M., Masselink, G., Losada, M.A., 2016a. Implications of delta retreat on wave propagation and longshore sediment transport—Guadalfeo case study (southern Spain). Mar. Geol. 382, 1–16.
Bergillos, R.J., Masselink, G., McCall, R.T., Ortega-Sánchez, M., 2016b. Modelling overwash vulnerability along mixed sand-gravel coasts with XBeach-G: case study of Playa Granada, southern Spain. Coastal Engineering Proceedings. vol. 1. pp. 13.
Bergillos, R.J., Ortega-Sánchez, M., Masselink, G., Losada, M.A., 2016c. Morpho-sedimentary dynamics of a micro-tidal mixed sand and gravel beach, Playa Granada, southern Spain. Mar. Geol. 379, 28–38.
Bergillos, R.J., Rodríguez-Delgado, C., Millares, A., Ortega-Sánchez, M., Losada, M.A., 2016d. Impact of river regulation on a Mediterranean delta: assessment of managed versus unmanaged scenarios. Water Resour. Res. 52, 5132–5148.
Bergillos, R.J., Masselink, G., Ortega-Sánchez, M., 2017a. Coupling cross-shore and longshore sediment transport to model storm response along a mixed sand–gravel coast under varying wave directions. Coast. Eng. 129, 93–104.
Bergillos, R.J., Rodríguez-Delgado, C., Ortega-Sánchez, M., 2017b. Advances in management tools for modeling artificial nourishments in mixed beaches. J. Mar. Syst. 172, 1–13.
Bergillos, R.J., Ortega-Sánchez, M., Losada, M.A., 2015a. Foreshore evolution of a mixed sand and gravel beach: the case of Playa Granada (Southern Spain). Proceedings of the 8th Coastal Sediments. World Scientific.
Bergillos, R.J., Rodríguez-Delgado, C., López-Ruiz, A., Millares, A., Ortega-Sánchez, M., Losada, M.A., 2015b. Recent human-induced coastal changes in the Guadalfeo river deltaic system (southern Spain). Proceedings of the 36th IAHR-International Association for Hydro-Environment Engineering and Research World Congress. http://89.31.100.18/∼iahrpapers/87178.pdf.
Carballo, R., Iglesias, G., 2013. Wave farm impact based on realistic wave-WEC interaction. Energy 51, 216–229.
Carballo, R., Sánchez, M., Ramos, V., Fraguela, J., Iglesias, G., 2015. The intra-annual variability in the performance of wave energy converters: a comparative study in N Galicia (Spain). Energy 82, 138–146.
Carballo, R., Sánchez, M., Ramos, V., Taveira-Pinto, F., Iglesias, G., 2014. A high resolution geospatial database for wave energy exploitation. Energy 68, 572–583.
Clément, A., McCullen, P., de O. Falcão, A.F., Fiorentino, A., Gardner, F., Hammarlund, K., Lemonis, G., Lewis, T., Nielsen, K., Petroncini, S., Pontes, M.-T., Schild, P., Sjöström, B.-O., Sørensen, H.C., Thorpe, T., 2002. Wave energy in Europe: current status and perspectives. Renew. Sust. Energ. Rev. 6, 405–431.
Contestabile, P., Di Lauro, E., Buccino, M., Vicinanza, D., 2017a. Economic assessment of Overtopping BReakwater for Energy Conversion (OBREC): a case study in Western Australia. Sustainability 9.
Contestabile, P., Iuppa, C., Di Lauro, E., Cavallaro, L., Andersen, T.L., Vicinanza, D., 2017b. Wave loadings acting on innovative rubble mound breakwater for overtopping wave energy conversion. Coast. Eng. 122, 60–74.
Cornett, A.M., 2008. A global wave energy resource assessment. The Eighteenth International Offshore and Polar Engineering Conference. International Society of Offshore and Polar Engineers.
Cruz, J., 2008. Ocean Wave Energy: Current Status and Future Perspectives. Springer Science & Business Media.
de O. Falcão, A.F., 2007. Modelling and control of oscillating-body wave energy converters with hydraulic power take-off and gas accumulator. Ocean Eng. 34, 2021–2032.
Deltares, 2014. XBeach-G GUI 1.0. User Manual. Delft, The Netherlands.
European Commission, 2007. A European Strategic Energy Technology Plan (Set-Plan): Towards a Low Carbon Future. Commission of the European Communities, Brussels.
Félix, A., Baquerizo, A., Santiago, J.M., Losada, M.A., 2012. Coastal zone management with stochastic multi-criteria analysis. J. Environ. Manag. 112, 252–266.
Feng, T., Zhou, W., Wu, S., Niu, Z., Cheng, P., Xiong, X., Li, G., 2018. Simulations of summertime fossil fuel CO_2 in the Guanzhong basin, China. Sci. Total Environ. 624, 1163–1170.
Fernandez, H., Iglesias, G., Carballo, R., Castro, A., Fraguela, J., Taveira-Pinto, F., Sanchez, M., 2012. The new wave energy converter WaveCat: concept and laboratory tests. Mar. Struct. 29, 58–70.
Gaete-Morales, C., Gallego-Schmid, A., Stamford, L., Azapagic, A., 2018. Assessing the environmental sustainability of electricity generation in Chile. Sci. Total Environ. 636, 1155–1170.
Hemer, M.A., Fan, Y., Mori, N., Semedo, A., Wang, X.L., 2013. Projected changes in wave climate from a multi-model ensemble. Nat. Clim. Chang. 3, 471.
Holthuijsen, L., Booij, N., Ris, R., 1993. A spectral wave model for the coastal zone. ASCE.
Iglesias, G., Carballo, R., 2011. Choosing the site for the first wave farm in a region: a case study in the Galician Southwest (Spain). Energy 36, 5525–5531.
Intergovernmental Panel on Climate Change, 2014. Climate Change 2014: Synthesis Report. IPCC, Geneva, Switzerland.
Iuppa, C., Cavallaro, L., Foti, E., Vicinanza, D., 2015. Potential wave energy production by different wave energy converters around Sicily. J. Renew. Sust. Energy 7, 061701.
López, I., Castro, A., Iglesias, G., 2015a. Hydrodynamic performance of an oscillating water column wave energy converter by means of particle imaging velocimetry. Energy 83, 89–103.
López, I., Pereiras, B., Castro, F., Iglesias, G., 2015b. Performance of OWC wave energy converters: influence of turbine damping and tidal variability. Int. J. Energy Res. 39, 472–483.
López, M., Veigas, M., Iglesias, G., 2015c. On the wave energy resource of Peru. Energy Convers. Manag. 90, 34–40.
López, I., Iglesias, G., 2014. Efficiency of OWC wave energy converters: a virtual laboratory. Appl. Ocean Res. 44, 63–70.
López, I., Pereiras, B., Castro, F., Iglesias, G., 2014. Optimisation of turbine-induced damping for an OWC wave energy converter using a RANS-VOF numerical model. Appl. Energy 127, 105–114.
López-Ruiz, A., Bergillos, R.J., Lira-Loarca, A., Ortega-Sánchez, M., 2018a. A methodology for the long-term simulation and uncertainty analysis of the operational lifetime performance of wave energy converter arrays. Energy 153, 126–135.
López-Ruiz, A., Bergillos, R.J., Raffo-Caballero, J.M., Ortega-Sánchez, M., 2018b. Towards an optimum design of wave energy converter arrays through an integrated approach of life cycle performance and operational capacity. Applied Energy 209, 20–32.

López-Ruiz, A., Bergillos, R.J., Ortega-Sánchez, M., 2016. The importance of wave climate forecasting on the decision-making process for nearshore wave energy exploitation. Appl. Energy 182, 191–203.
Losada, M.A., Baquerizo, A., Ortega-Sánchez, M., Ávila, A., 2011. Coastal evolution, sea level, and assessment of intrinsic uncertainty. J. Coast. Res. 59, 218–228.
Margheritini, L., Vicinanza, D., Frigaard, P., 2009. SSG wave energy converter: design, reliability and hydraulic performance of an innovative overtopping device. Renew. Energy 34, 1371–1380.
McCall, R.T., Masselink, G., Poate, T.G., Roelvink, J.A., Almeida, L.P., 2015. Modelling the morphodynamics of gravel beaches during storms with XBeach-G. Coast. Eng. 103, 52–66.
McCall, R.T., Masselink, G., Poate, T.G., Roelvink, J.A., Almeida, L.P., Davidson, M., Russell, P.E., 2014. Modelling storm hydrodynamics on gravel beaches with XBeach-G. Coast. Eng. 91, 231–250.
Medina-López, E., Bergillos, R., Moñino, A., Clavero, M., Ortega-Sánchez, M., 2017. Effects of seabed morphology on oscillating water column wave energy converters. Energy 135, 659–673.
Mendoza, E., Silva, R., Zanuttigh, B., Angelelli, E., Andersen, T.L., Martinelli, L., Nørgaard, J.Q.H., Ruol, P., 2014. Beach response to wave energy converter farms acting as coastal defence. Coast. Eng. 87, 97–111.
Millar, D., Smith, H., Reeve, D., 2007. Modelling analysis of the sensitivity of shoreline change to a wave farm. Ocean Eng. 34, 884–901.
Millares, A., Polo, M.J., Moñino, A., Herrero, J., Losada, M.A., 2014. Bedload dynamics and associated snowmelt influence in mountainous and semiarid alluvial rivers. Geomorphology 206, 330–342.
Ortega-Sánchez, M., Bergillos, R.J., López-Ruiz, A., Losada, M.A., 2017. Morphodynamics of Mediterranean Mixed Sand and Gravel Coasts. Springer.
Pagán, J., López, I., Aragonés, L., Garcia-Barba, J., 2017. The effects of the anthropic actions on the sandy beaches of Guardamar del Segura, Spain. Sci. Total Environ. 601-602, 1364–1377.
Palha, A., Mendes, L., Fortes, C.J., Brito-Melo, A., Sarmento, A., 2010. The impact of wave energy farms in the shoreline wave climate: Portuguese pilot zone case study using Pelamis energy wave devices. Renew. Energy 35, 62–77.
Pérez-Collazo, C., Greaves, D., Iglesias, G., 2015. A review of combined wave and offshore wind energy. Renew. Sust. Energy Rev. 42, 141–153.
Rodriguez-Delgado, C., Bergillos, R.J., Iglesias, G., 2019. Dual wave energy converter farms and coastline dynamics: the role of inter-device spacing. Sci. Total Environ. 646, 1241–1252.
Rodriguez-Delgado, C., Bergillos, R.J., Ortega-Sánchez, M., Iglesias, G., 2018a. Protection of gravel-dominated coasts through wave farms: layout and shoreline evolution. Sci. Total Environ. 636, 1541–1552.
Rodriguez-Delgado, C., Bergillos, R.J., Ortega-Sánchez, M., Iglesias, G., 2018b. Wave farm effects on the coast: the alongshore position. Sci. Total Environ. 640, 1176–1186.
Sánchez-Arcilla, A., García-León, M., Gracia, V., Devoy, R., Stanica, A., Gault, J., 2016. Managing coastal environments under climate change: pathways to adaptation. Sci. Total Environ. 572, 1336–1352.
Shafiee, S., Topal, E., 2009. When will fossil fuel reserves be diminished? Energy Policy 37, 181–189.
Silva, D., Bento, A.R., Martinho, P., Soares, C.G., 2015. High resolution local wave energy modelling in the Iberian Peninsula. Energy 91, 1099–1112.
Viviano, A., Naty, S., Foti, E., Bruce, T., Allsop, W., Vicinanza, D., 2016. Large-scale experiments on the behaviour of a generalised oscillating water column under random waves. Renew. Energy 99, 875–887.
Vousdoukas, M.I., Voukouvalas, E., Annunziato, A., Giardino, A., Feyen, L., 2016. Projections of extreme storm surge levels along Europe. Clim. Dyn. 47, 3171–3190.